

Electronic Supplementary Information

A novel and simple solvent-dependent fluorescent probe based on a click generated 8-aminoquinoline–steroid conjugate for multi-detection of Cu(II), oxalate and pyrophosphate

Zhen Zhang*, Yuan Zou and Chengquan Deng

Department of Applied Chemistry, School of Science, Xi'an Jiaotong University, Xi'an 710049, China. E-mail: zzlinda@mail.xjtu.edu.cn; Fax: +86 29 82668559; Tel: +86 29 82663914.

Contents

1. ^1H NMR spectrum of compound **2**
2. ^1H NMR spectrum of compound **3**
3. ^1H NMR, ^{13}C NMR, and HR-ESI-MS spectra of probe **1**
4. UV-vis absorption spectra of probe **1** with different levels of Cu^{2+}
5. UV-vis absorption spectra of probe **1** with different metal ions
6. Effects of CH_3CN content on the fluorescence response of probe **1** to Cu^{2+}
7. Effects of pH on the fluorescence response of probe **1** to Cu^{2+}
8. Time-dependent fluorescence response of probe **1** upon addition of Cu^{2+}
9. UV-vis absorption spectra of probe **1** with different anions
10. UV-vis absorption spectra of probe **1** with different levels of $\text{C}_2\text{O}_4^{2-}/\text{P}_2\text{O}_7^{4-}$
11. Effects of DMSO content on the fluorescence response of probe **1** to $\text{C}_2\text{O}_4^{2-}/\text{P}_2\text{O}_7^{4-}$
12. Effects of pH on the fluorescence response of probe **1** to $\text{C}_2\text{O}_4^{2-}/\text{P}_2\text{O}_7^{4-}$
13. Time-dependent fluorescence response of probe **1** upon addition of $\text{C}_2\text{O}_4^{2-}/\text{P}_2\text{O}_7^{4-}$
14. ^1H NMR spectra of probe **1** measured before and after addition of Cu^{2+}
15. The reversibility of probe **1** for Cu^{2+} detection
16. The reversibility of probe **1** for $\text{C}_2\text{O}_4^{2-}/\text{P}_2\text{O}_7^{4-}$ detection
17. Comparison of the recently reported multi-detection probes for Cu^{2+} , $\text{C}_2\text{O}_4^{2-}$ and $\text{P}_2\text{O}_7^{4-}$

1. ^1H NMR spectrum of compound **2**

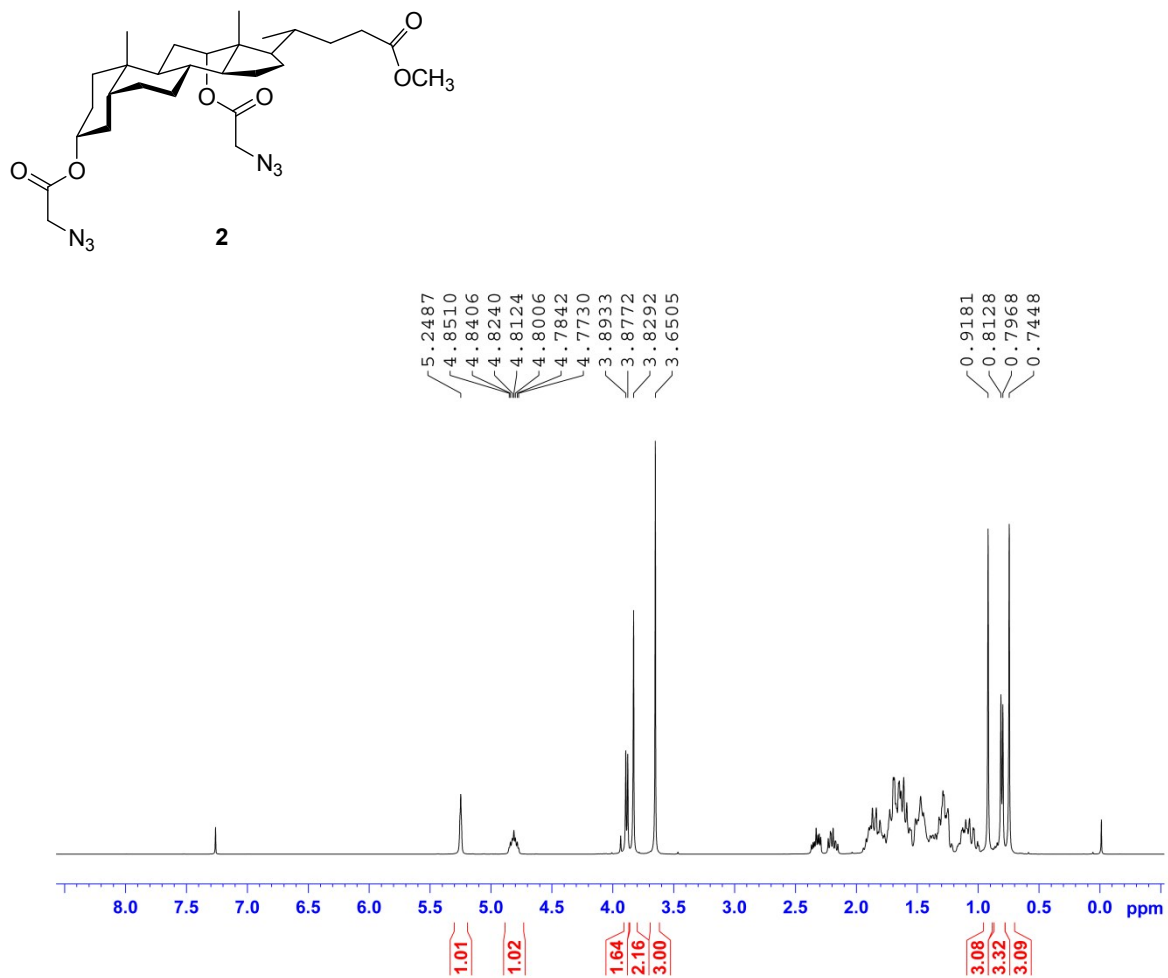


Fig. S1 ^1H NMR spectrum of compound **2**.

2. ^1H NMR spectrum of compound **3**

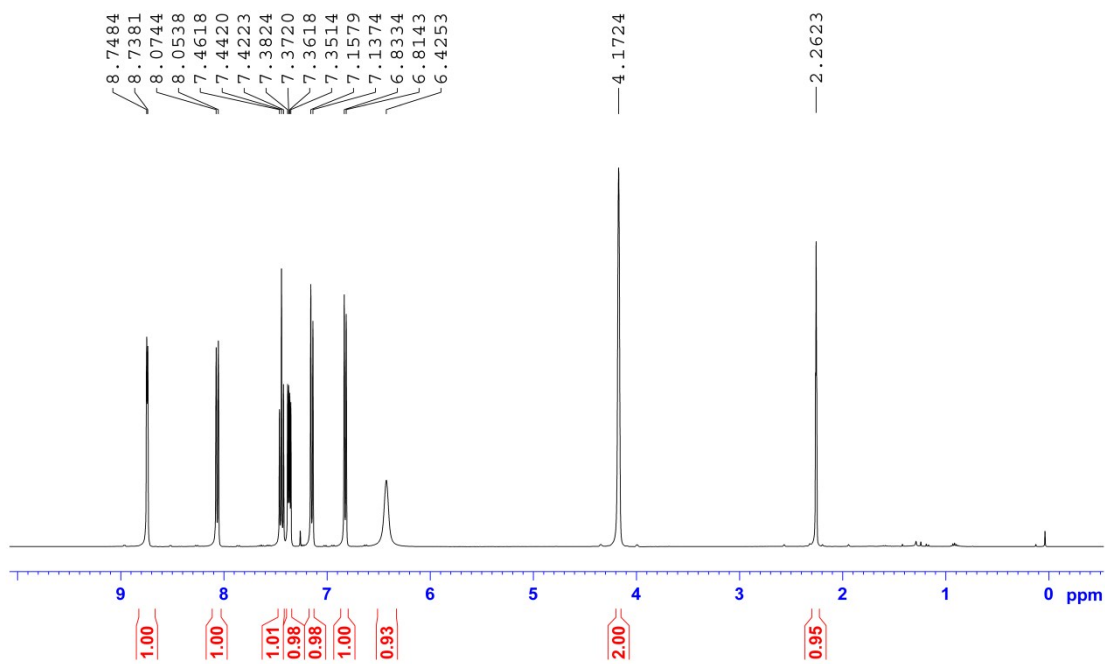
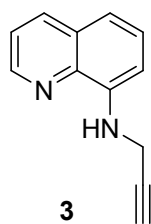


Fig. S2 ^1H NMR spectrum of compound **3**.

3. ^1H NMR, ^{13}C NMR, and HR-ESI-MS spectra of probe **1**

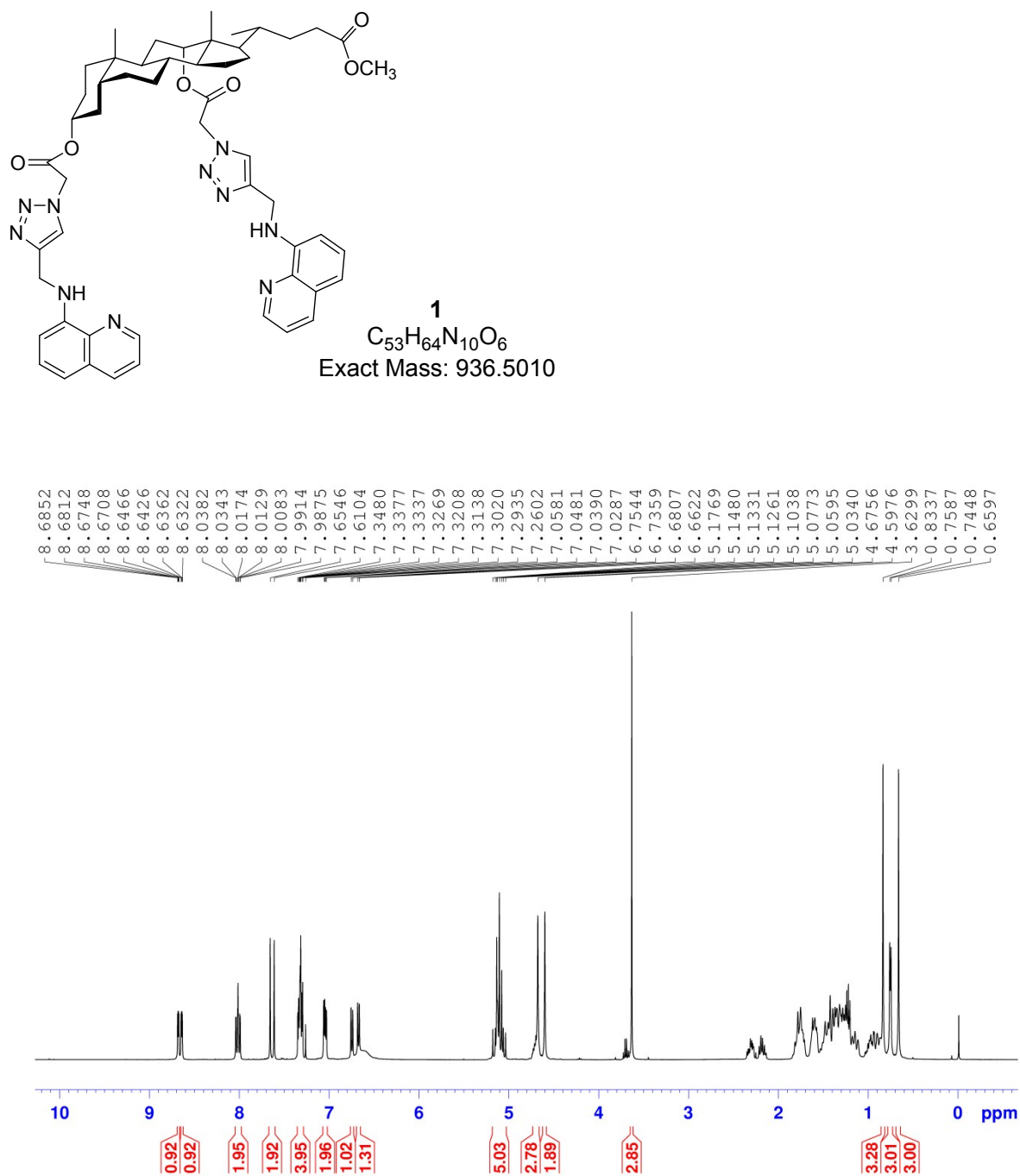


Fig. S3 ^1H NMR spectrum of probe **1**.

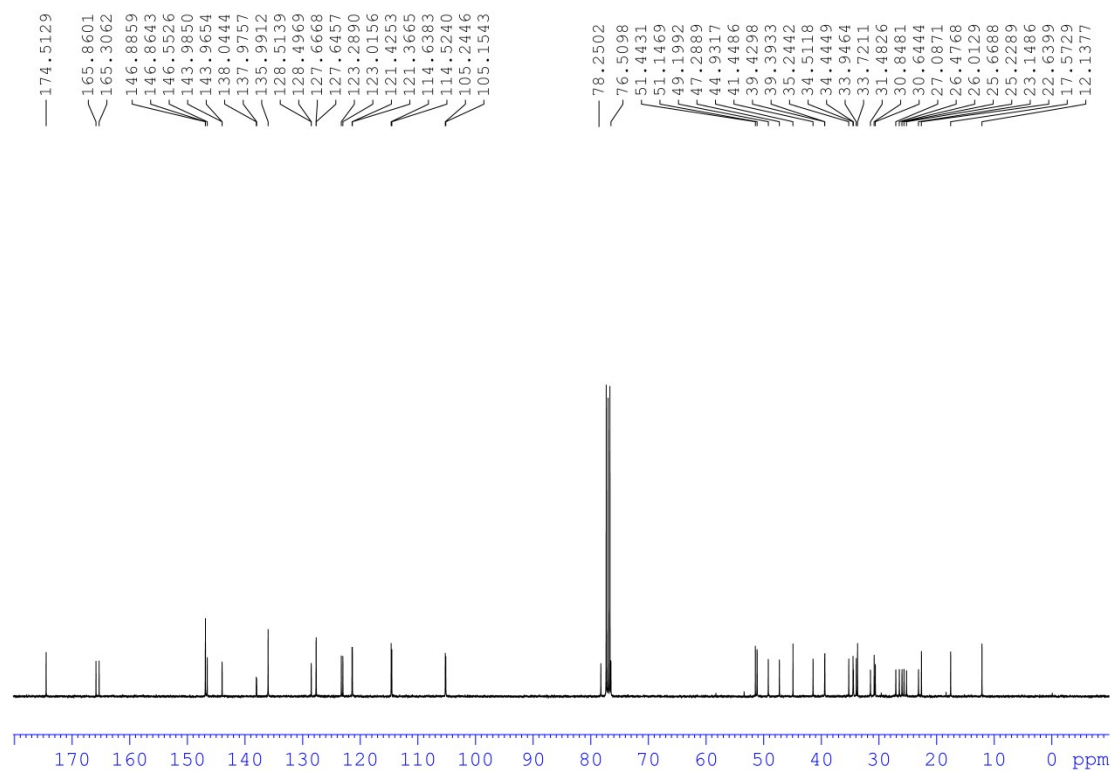


Fig. S4 ^{13}C NMR spectrum of probe 1.

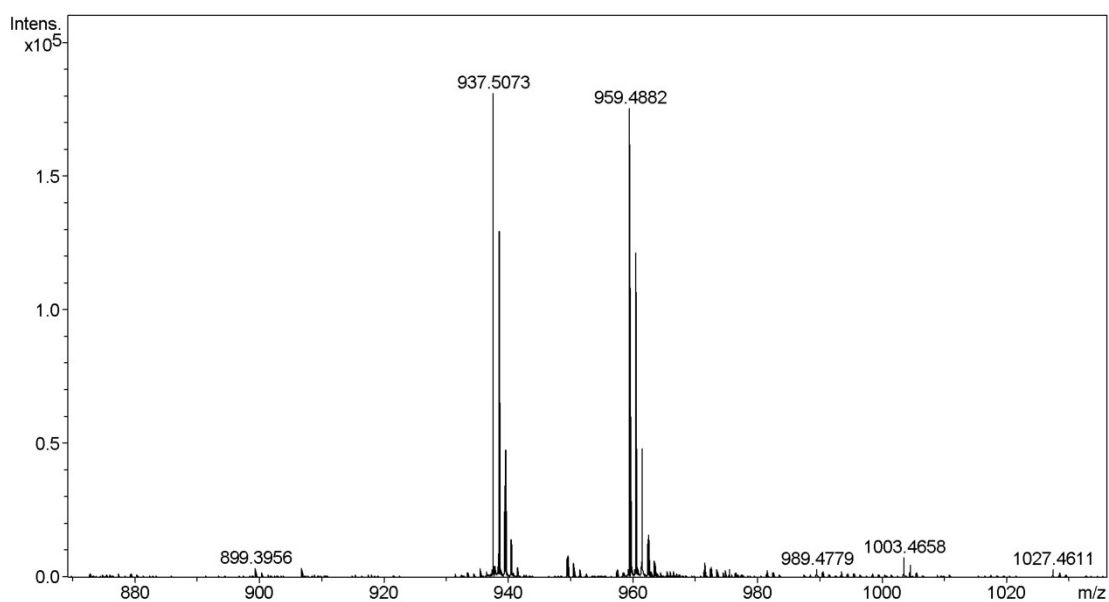


Fig. S5 HR-ESI-MS spectrum of probe 1.

4. UV-vis absorption spectra of probe **1** with different levels of Cu^{2+}

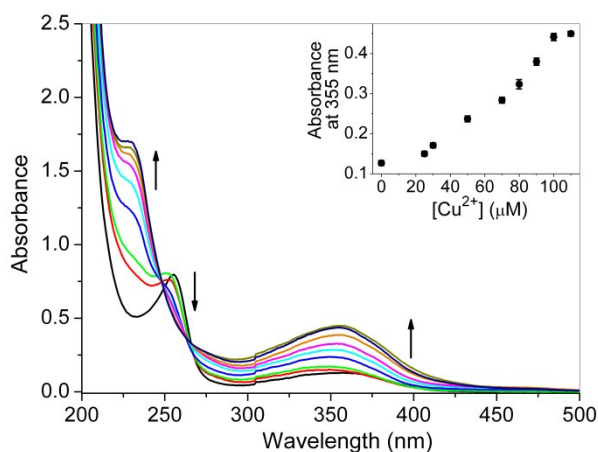


Fig. S6 UV-vis absorption spectra of probe **1** (20 μM) with different levels of Cu^{2+} (from bottom to top: 0, 25, 30, 50, 70, 80, 90, 100 and 110 μM) in $\text{CH}_3\text{CN}-\text{H}_2\text{O}$ (99/1, v/v, 10 mM HEPES, pH 7.2). Inset: absorbance changes of probe **1** at 355 nm as a function of Cu^{2+} concentration.

5. UV-vis absorption spectra of probe **1** with different metal ions

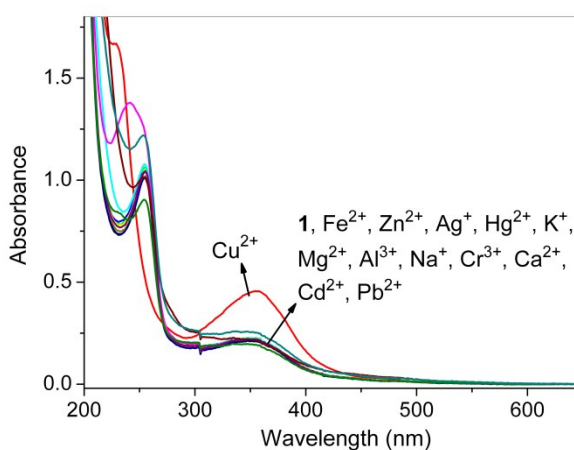


Fig. S7 UV-vis absorption spectra of probe **1** (20 μM) with different metal ions (100 μM) in $\text{CH}_3\text{CN}-\text{H}_2\text{O}$ (99/1, v/v, 10 mM HEPES, pH 7.2).

6. Effects of CH₃CN content on the fluorescence response of probe **1** to Cu²⁺

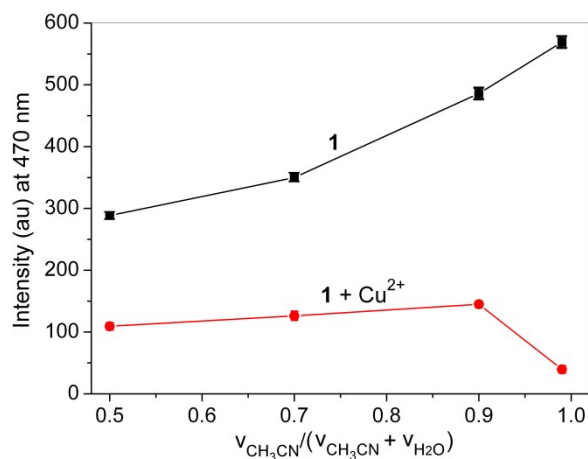


Fig. S8 Effects of CH₃CN content on the fluorescence intensity of probe **1** (20 μM) at 470 nm in the absence and presence of Cu²⁺ (100 μM) in aqueous solution (10 mM HEPES, pH 7.2). $\lambda_{\text{ex}} = 350$ nm.

7. Effects of pH on the fluorescence response of probe **1** to Cu²⁺

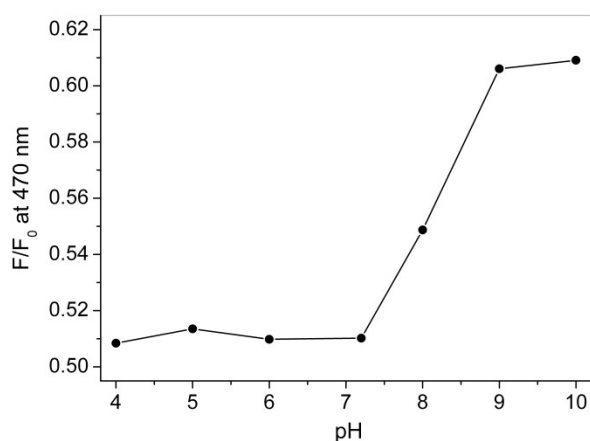


Fig. S9 Fluorescence intensity ratios of probe **1** (20 μM) at 470 nm after (F) and before (F₀) addition of Cu²⁺ (50 μM) in CH₃CN–H₂O (99/1, v/v, 10 mM HEPES) at various pH values (from 4.0 to 10.0). $\lambda_{\text{ex}} = 350$ nm.

8. Time-dependent fluorescence response of probe **1** upon addition of Cu^{2+}

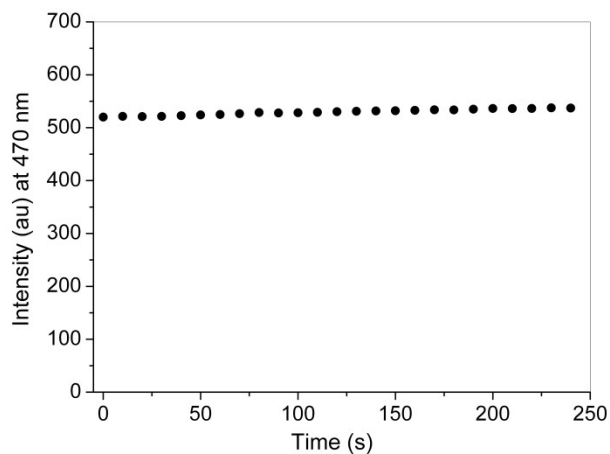


Fig. S10 Time course of the fluorescence intensity changes of probe **1** (20 μM) at 470 nm upon addition of Cu^{2+} (10 μM) in $\text{CH}_3\text{CN-H}_2\text{O}$ (99/1, v/v, 10 mM HEPES, pH 7.2). $\lambda_{\text{ex}} = 350$ nm.

9. UV-vis absorption spectra of probe **1** with different anion

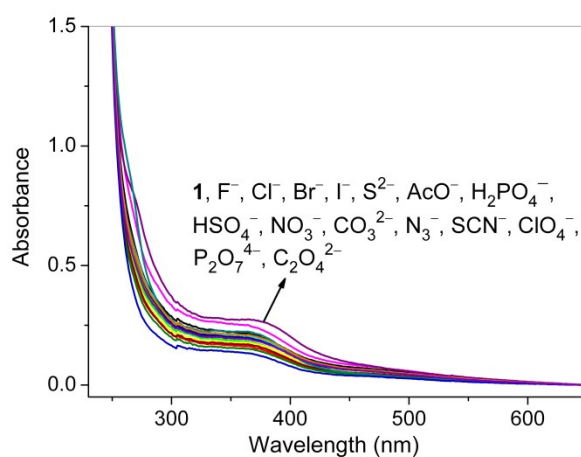


Fig. S11 UV-vis absorption spectra of probe **1** (20 μM) with different anions (30 μM) in $\text{DMSO-H}_2\text{O}$ (1/1, v/v, 10 mM HEPES, pH 7.2).

10. UV-vis absorption spectra of probe **1** with different levels of $\text{C}_2\text{O}_4^{2-}/\text{P}_2\text{O}_7^{4-}$

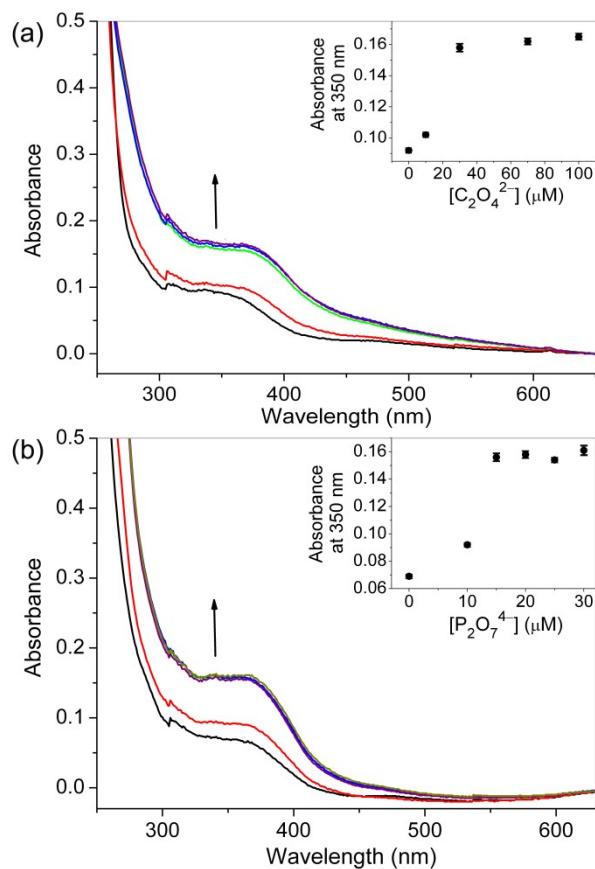


Fig. S12 UV-vis absorption spectra of probe **1** (20 μM) with different levels of (a) C₂O₄²⁻ (from bottom to top: 0, 10, 30, 70 and 100 μM) and (b) P₂O₇⁴⁻ (from bottom to top: 0, 10, 15, 20, 25 and 30 μM) in DMSO-H₂O (1/1, v/v, 10 mM HEPES, pH 7.2).

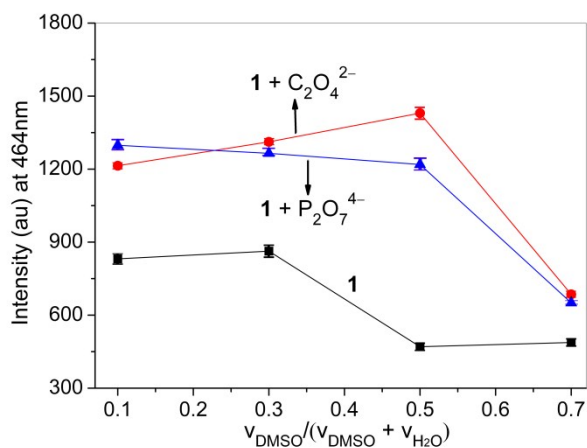


Fig. S13 Effects of DMSO content on the fluorescence intensity of probe **1** (20 μM) at 464 nm in the absence and presence of $\text{C}_2\text{O}_4^{2-}/\text{P}_2\text{O}_7^{4-}$ (50 μM) in aqueous solution (10 mM HEPES, pH 7.2). $\lambda_{\text{ex}} = 350$ nm.

12. Effects of pH on the fluorescence response of probe **1** to $\text{C}_2\text{O}_4^{2-}/\text{P}_2\text{O}_7^{4-}$

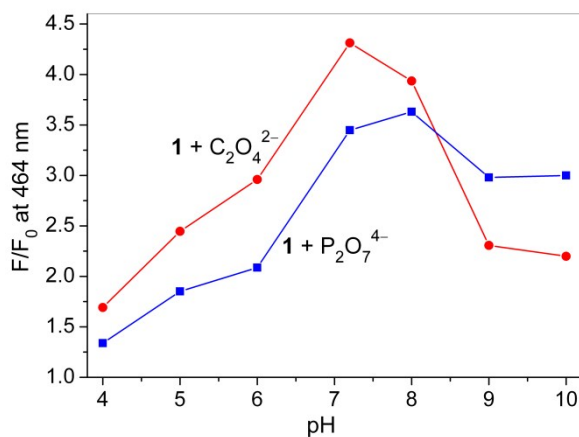


Fig. S14 Fluorescence intensity ratios of probe **1** (20 μM) at 464 nm after (F) and before (F_0) addition of $\text{C}_2\text{O}_4^{2-}/\text{P}_2\text{O}_7^{4-}$ (50 μM) in DMSO– H_2O (1/1, v/v, 10 mM HEPES) at various pH values (from 4.0 to 10.0). $\lambda_{\text{ex}} = 350$ nm.

13. Time-dependent fluorescence response of probe **1** upon addition of $\text{C}_2\text{O}_4^{2-}/\text{P}_2\text{O}_7^{4-}$

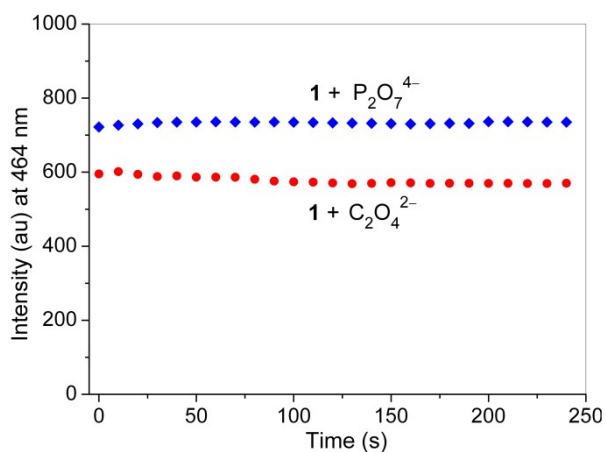


Fig. S15 Time course of the fluorescence intensity changes of probe **1** (20 μM) at 464 nm upon addition of $\text{C}_2\text{O}_4^{2-}/\text{P}_2\text{O}_7^{4-}$ (10 μM) in DMSO– H_2O (1/1, v/v, 10 mM HEPES, pH 7.2). $\lambda_{\text{ex}} = 350$ nm.

14. ^1H NMR spectra of probe **1** measured before and after addition of Cu^{2+}

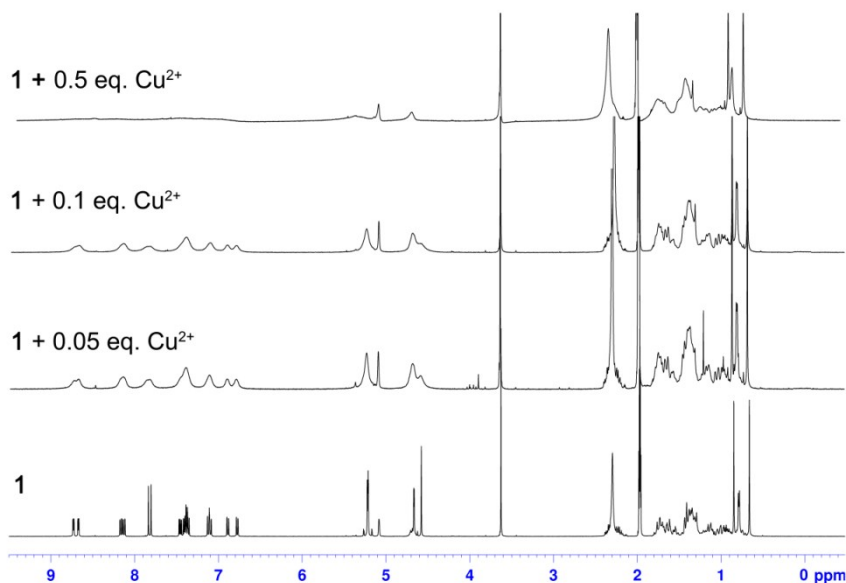


Fig. S16 ^1H NMR spectra of probe **1** (10 mM) measured before and after addition of Cu^{2+} (0.05, 0.1 and 0.5 equivalent) in $\text{CD}_3\text{CN}-\text{D}_2\text{O}$ (99/1, v/v).

15. The reversibility of probe **1** for Cu^{2+} detection

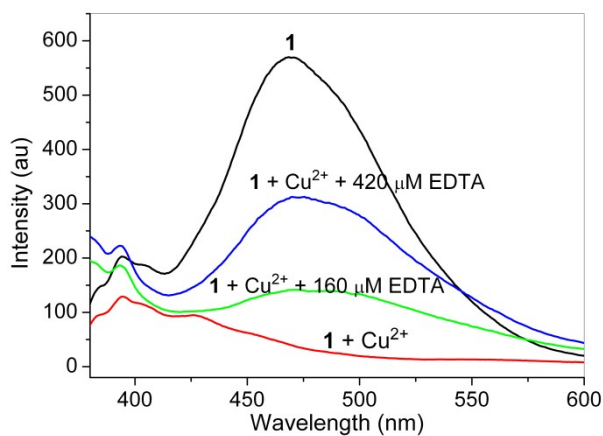


Fig. S17 Fluorescence spectra of probe **1**-Cu²⁺ complex with different levels of EDTA in CH₃CN-H₂O (99/1, v/v, 10 mM HEPES, pH 7.2). Probe **1** (20 M), Cu²⁺ (100 μM). λ_{ex} = 350 nm.

16. The reversibility of probe **1** for C₂O₄²⁻/P₂O₇⁴⁻ detection

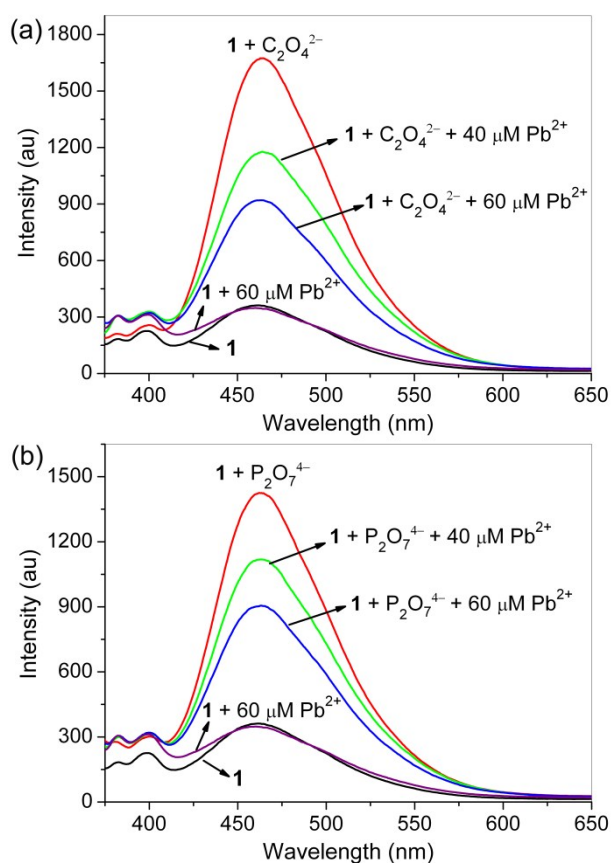
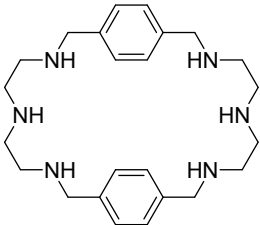
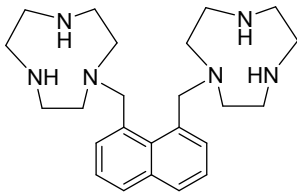
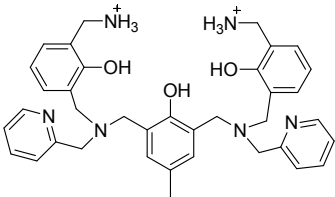
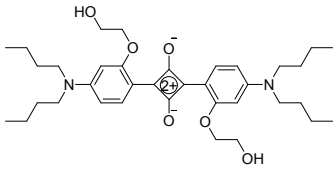
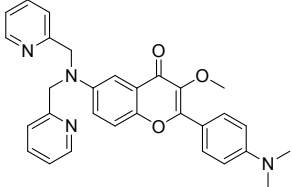
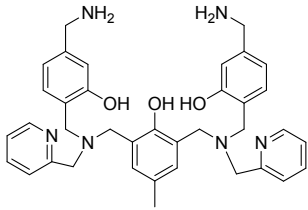
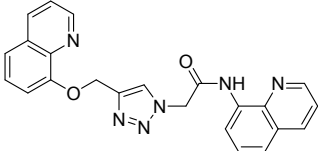
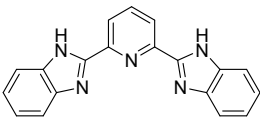
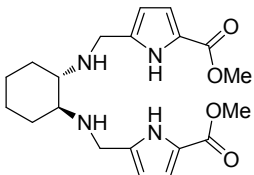
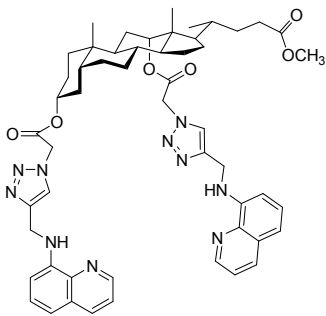


Fig. S18 Fluorescence spectra of (a) probe **1**-C₂O₄²⁻ complex and (b) probe **1**-P₂O₇⁴⁻ complex with different levels of Pb²⁺ in DMSO-H₂O (1/1, v/v, 10 mM HEPES, pH 7.2). Probe **1** (20 M), C₂O₄²⁻/P₂O₇⁴⁻ (100 μM). λ_{ex} = 350 nm.

17. **Table S1.** Comparison of the recently reported multi-detection probes for Cu^{2+} , $\text{C}_2\text{O}_4^{2-}$ and $\text{P}_2\text{O}_7^{4-}$

Probe	Detection mode and properties	K_a	Detection limit	Response time
carbon dots <i>Mater. Lett.</i> , 2014, 115 , 233	fluorescent turn-off/on for sequential detection of Cu^{2+} and $\text{C}_2\text{O}_4^{2-}$ (based on Cu^{2+} displacement approach) in Tris buffer solution, $\lambda_{\text{ex}}/\lambda_{\text{em}}$ 470/543 nm, quantitative detection ranged from 10–90 μM for Cu^{2+} , and 10–70 μM for $\text{C}_2\text{O}_4^{2-}$	no data	1 μM for $\text{C}_2\text{O}_4^{2-}$	rapid, no data
 <i>Chem. Commun.</i> , 2012, 48 , 6951	by fluorescent indicator (fluorescein, $\lambda_{\text{ex}}/\lambda_{\text{em}}$ 470/510 nm, and eosin Y, $\lambda_{\text{ex}}/\lambda_{\text{em}}$ 490/540 nm) displacement assays, macrocyclic(L)– Cu^{2+} complex formed an ensemble with $\text{C}_2\text{O}_4^{2-}$ and showed off-on fluorescent sensing for $\text{C}_2\text{O}_4^{2-}$ in water at neutral pH with quantitative detection ranged from 0–5 μM using Cu_2L –Eosin Y	$> 10^7 \text{ M}^{-1}$ for $\text{C}_2\text{O}_4^{2-}$	0.079 μM for $\text{C}_2\text{O}_4^{2-}$ by Cu_2L –Eosin Y	no data
 <i>J. Am. Chem. Soc.</i> , 2008, 130 , 12606	by the fluorescent indicator eosin Y displacement, a dimacrocyclic– Cu^{2+} complex could form an ensemble with $\text{C}_2\text{O}_4^{2-}$ and showed off-on fluorescent sensing ($\lambda_{\text{ex}}/\lambda_{\text{em}}$ 524/537 nm) for $\text{C}_2\text{O}_4^{2-}$ in water at neutral pH	$(1.3 \pm 0.1) \times 10^5 \text{ M}^{-1}$ for $\text{C}_2\text{O}_4^{2-}$	no data	no data
 <i>Sens. Actuators B</i> , 2016, 233 , 591	by indicator (pyrocatechol violet, colorimetric indicator, ratio of A_{655}/A_{444} ; esculetine, fluorescent indicator, $\lambda_{\text{ex}}/\lambda_{\text{em}}$ 380/465 nm) displacement, a dinuclear– Cu^{2+} complex with two ammonium arms formed an ensemble with $\text{P}_2\text{O}_7^{4-}$, showing color changes and off-on fluorescence in aqueous solution	by the UV indicator, $8.55 \times 10^6 \text{ M}^{-1}$ for $\text{P}_2\text{O}_7^{4-}$	0.15 μM for $\text{P}_2\text{O}_7^{4-}$ by fluorescence assay	no data

Probe	Detection mode and properties	K_a	Detection limit	Response time
 <p><i>Sens. Actuators B</i>, 2016, 233, 550</p>	<p>a squaraine-based fluorescent probe chelated Cu^{2+} and showed on-off sensing ($\lambda_{\text{ex}}/\lambda_{\text{em}}$ 620/670 nm, quantitative detection range 0.5–3.5 μM) in MeCN–H_2O (9/1, v/v). $\text{P}_2\text{O}_7^{4-}$ extracted Cu^{2+} from the probe–Cu^{2+} complex and restored the spectral signal of free probe (quantitative detection range 0–25 μM)</p>	no data	near 15 nM for Cu^{2+} , and 0.072 μM for $\text{P}_2\text{O}_7^{4-}$	no data
 <p><i>Sens. Actuators B</i>, 2016, 229, 131</p>	<p>a flavonoid-based probe exhibited fluorescence quenching ($\lambda_{\text{ex}}/\lambda_{\text{em}}$ 390/510 nm) to Cu^{2+} with quantitative detection ranged from 0–10 μM in DMSO–H_2O (v/v = 9/1, 0.1 mM PBS, pH 7.4). Moreover, the probe–Cu^{2+} complex could also be used for secondary sensing of $\text{P}_2\text{O}_7^{4-}$ based on Cu^{2+} displacement approach with fluorescence turn-on behavior</p>	no data	lower than 100 nM for Cu^{2+}	no data
<p>carbon quantum dots with rich carboxyl groups on the surface</p> <p><i>Biosens. Bioelectron.</i>, 2015, 68, 675</p>	<p>richness of carboxyl on the surface of carbon quantum dots enables aggregation caused fluorescence quenching by Cu^{2+}, and the competitive interaction among carboxyl, Cu^{2+} and $\text{P}_2\text{O}_7^{4-}$ endows disaggregation induced fluorescence enhancement, $\lambda_{\text{ex}}/\lambda_{\text{em}}$ 452/525 nm</p>	no data	0.3 μM for $\text{P}_2\text{O}_7^{4-}$	real-time
 <p><i>Org. Lett.</i>, 2014, 16, 2220</p>	<p>by colorimetric indicator (pyrocatechol violet, ratio of A_{630}/A_{444}) displacement, a dinuclear–Cu^{2+} complex with ammonium moieties formed an ensemble with $\text{P}_2\text{O}_7^{4-}$, showing colorimetric changes in aqueous solution</p>	$5.75 \times 10^6 \text{ M}^{-1}$ for $\text{P}_2\text{O}_7^{4-}$	no data	no data

Probe	Detection mode and properties	K_a	Detection limit	Response time
 <p><i>Tetrahedron Lett.</i>, 2013, 54, 5948</p>	<p>a quinoline derivative was used as a fluorescent probe for sequential sensing ($\lambda_{ex}/\lambda_{em}$ 305/412 nm) of Cu^{2+} and $\text{P}_2\text{O}_7^{4-}$ in DMSO–H_2O (1/1, v/v, 20 mM HEPES, pH 7.4). The probe displayed high selectivity to Cu^{2+} (quantitative detection range 0–20 μM), and the probe–Cu^{2+} showed high selectivity to $\text{P}_2\text{O}_7^{4-}$ (quantitative detection range 1–20 μM) with emission recovery of the free probe</p>	1.59×10^7 M^{-1} for Cu^{2+}	4.47 μM for Cu^{2+} , and 3.16 μM for $\text{P}_2\text{O}_7^{4-}$	no data
 <p><i>Biosens. Bioelectron.</i>, 2011, 30, 282</p>	<p>a turn-on fluorescent probe ($\lambda_{ex}/\lambda_{em}$ 280/395 nm) based on Cu^{2+} complex of 2,6-bis(2-benzimidazolyl)pyridine was developed for $\text{P}_2\text{O}_7^{4-}$, due to the formation of a ternary complex of probe–Cu^{2+}–$\text{P}_2\text{O}_7^{4-}$, with quantitative detection range of 3–90 μM at a neutral pH</p>	no data	no data	no data
 <p><i>J. Fluoresc.</i>, 2011, 21, 701</p>	<p>constructed by a copper complex (receptor) and eosin Y (indicator), an ensemble displayed fluorescent off-on ($\lambda_{ex}/\lambda_{em}$ 523/543 nm) recognition of $\text{P}_2\text{O}_7^{4-}$ in water at pH 7.4</p>	1.17×10^5 M^{-1} for $\text{P}_2\text{O}_7^{4-}$	no data	no data
 <p><i>This work</i></p>	<p>fluorescence quenching ($\lambda_{ex}/\lambda_{em}$ 350/470 nm) upon binding to Cu^{2+} in CH_3CN–H_2O (99/1, v/v, 10 mM HEPES, pH 7.2), and fluorescent enhanced response ($\lambda_{ex}/\lambda_{em}$ 350/464 nm) toward $\text{C}_2\text{O}_4^{2-}$ and $\text{P}_2\text{O}_7^{4-}$ in DMSO–H_2O (1/1, v/v, 10 mM HEPES, pH 7.2)</p>	3.28×10^3 M^{-1} for Cu^{2+} , 2.23×10^4 M^{-1} for $\text{C}_2\text{O}_4^{2-}$ and 4.96×10^4 M^{-1} for $\text{P}_2\text{O}_7^{4-}$	0.12 μM for Cu^{2+} , 0.28 μM for $\text{C}_2\text{O}_4^{2-}$ and 0.55 μM for $\text{P}_2\text{O}_7^{4-}$	completed within several seconds